Archives of Virology (2022) 167:1841–1854
https://doi.org/10.1007/s00705-022-05499-3

ORIGINAL ARTICLE

MicroRNA-223 downregulation promotes HBx-induced podocyte pyroptosis by targeting the NLRP3 inflammasome

Yani Yu[1] · Hui Dong[2] · Yue Zhang[3] · Jingyi Sun[1] · Baoshuang Li[1] · Yueqi Chen[1] · Moxuan Feng[1] · Xiaoqian Yang[1] · Shengbo Gao[4] · Wei Jiang[1]

Received: 27 December 2021 / Accepted: 21 April 2022 / Published online: 22 June 2022

Abstract

Hepatitis B virus (HBV) and its related protein, HBV X (HBx), play an important role in podocyte injury in HBV-associated glomerulonephritis (HBV-GN). The microRNA MiR-223 is expressed in several diseases, including HBV-associated disease, while the nucleotide-binding oligomerization domain-like receptor protein 3 (NLRP3) inflammasome plays a major role in pyroptosis. In this study, we investigated the function and mechanism of action of miR-223 in HBx-induced podocyte pyroptosis. A quantitative real-time reverse transcription polymerase chain reaction (qRT-PCR) assay showed that miR-223 was downregulated in HBx-transfected podocytes. Transfection with an miR-223 mimic abolished the expression of the NLRP3 inflammasome and the cytokines that are released as a result of NLRP3 overexpression. Moreover, transfection with HBx and NLRP3 overexpression plasmids increased the expression of pyroptosis-related proteins, especially in the presence of miR-223 inhibitors. Thus, miR-223 downregulation plays an important role in HBx-induced podocyte pyroptosis by targeting the NLRP3 inflammasome, suggesting that miR-223 is a potential therapeutic target for alleviating HBV-GN inflammation.

Introduction

Hepatitis B virus (HBV) has been spreading widely in China for a long period of time, and HBV-related glomerulonephritis (HBV-GN) is one of the major secondary kidney diseases in the country [1]. Interestingly, the course of HBV-GN inevitably results in podocyte injury, which in turn aggravates disease progression. Previous studies have shown that the expression of HBV proteins, especially the HBV X protein (HBx), has crucial effects on the pathogenesis of HBV-GN [2, 3]. However, the specific mechanism of HBV-GN pathogenesis remains unclear, and the cellular events leading to podocyte injury need to be investigated.

Pyroptosis exhibits the common characteristics of programmed cell death, including DNA breakage and cell swelling and rupture. Notably, pyroptosis is associated with the activation of the nucleotide-binding oligomerization domain-like receptor protein 3 (NLRP3) inflammasome involving caspase-1, which leads to a strong inflammatory response [4]. On the one hand, activated caspase-1 cleaves the interleukin (IL)-1β and IL-18 precursors, producing mature cytokines. On the other hand, pyroptosis leads to cytosis and the release of cytoplasmic contents, exacerbating the effect of inflammation [5]. Many studies have shown that the NLRP3 inflammasome, a complex consisting mainly of NLRP3, apoptosis-associated speck-like protein (ASC), and pro-caspase-1, is involved not only in the inflammatory progression of myocardial ischemia-reperfusion injury and sepsis-induced liver impairment, among others, but also in renal inflammation in chronic kidney disease (CKD) [6–9]. A cohort study of half a million Chinese adults indicated that chronic HBV infection increases the risk of CKD, especially in men [10]. However, the underlying mechanism by which pyroptosis acts during the development of HBV-GN requires clarification.

MicroRNAs (miRNAs) are a class of endogenous, non-coding single-stranded RNA molecules approximately 19-22

Handling Editor: Zhongjie Shi.

Yani Yu and Hui Dong contributed equally to this work.

✉ Wei Jiang
jiangwei866@qdu.edu.cn

1 Department of Nephrology, The Affiliated Hospital of Qingdao University, Qingdao 266003, Shandong, China

2 Health Management Center, The Affiliated Hospital of Qingdao University, Qingdao 266003, Shandong, China

3 Department of Stomatology, Qingdao Municipal Hospital Group, Qingdao 266003, Shandong, China

4 Department of Nephrology, The People's Hospital of Changle County, Weifang 262400, Shandong, China

nucleotides in length that inhibit the translation of target mRNAs by binding to their 3′-untranslated region (UTR), thereby negatively regulating gene expression [11]. Numerous studies have shown that miRNAs control several physiological and pathological processes, such as body growth, viral infection, and cancer metastasis [12–14]. miRNAs, which have potential as biomarkers and therapeutic agents, are key regulatory factors in injury processes, including podocyte apoptosis and inflammation [15]. However, their involvement in HBx-induced podocyte pyroptosis remains unclear.

In this study, we investigated the function and potential mechanism of miR-223 in HBx-induced podocyte pyroptosis and confirmed that miR-223 affects HBV-GN pathogenesis and podocyte damage by regulating the NLRP3 signaling pathway. Thus, miR-223 may be a potential treatment target for HBV-GN.

Materials and methods

Lentivirus infection and siRNA transfection

HBx-overexpressing lentiviruses, negative control lentiviruses, and NLRP3 siRNA (si-NLRP3) were synthesized by Shanghai Genechem Co., Ltd. Prior to transfection, podocytes at a density of 120,000 cells per well were seeded in 6-well plates and allowed to grow overnight. Then, the original medium was replaced with fresh medium (2 ml) containing polybrene (40 µl), and a suspension of the HBx-overexpressing lentivirus (7 µl) was added to the plates. After 24 h at 37 °C, the medium containing the lentivirus was removed and fresh medium was added. At 72 h post-transfection, the podocytes were examined by immunofluorescence assay (see below) to determine the efficiency of lentiviral infection of the target cells. In addition, the podocytes were transfected with negative control lentiviruses or si-NLRP3 as described above.

Podocytes were plated in 6-well culture plates in Opti-MEM (#YC-3039; Shanghai Yuchun Biotechnology Co., Ltd.). After reaching 50% confluence, podocytes were transfected with synthetic mature miR-223 (miR-223 mimic), antagomir antisense to mature miR-223 (miR-223 inhibitor), or a scrambled control transcript that served as a negative control (miR-NC). For overexpression of miR-223 in podocytes, the miR-223 mimic was dissolved in a transfection medium mixture of Opti-MEM and Lipofectamine 2000 (#11668-019; Invitrogen) at a working concentration of 50 nM according to the manufacturer's protocol. The transfection mixture (500 µl per well) was added to the cells, which were then incubated at 37 °C with 5% CO_2 for 48 h and the medium was replaced with fresh medium 6 h after transfection. After 1 day, the expression levels of miR-223 were measured by qRT-PCR. Successfully transfected podocytes were used for the further experiments. The miR-223 inhibitor and miR-NC were prepared using the same method.

Plasmid construction and transfection

GV146 vectors were purchased from Shanghai Genechem Co., Ltd. and used to construct the NLRP3 overexpression plasmids. Reactions were carried out according to the instructions of the manufacturer of PrimeSTAR HS DNA polymerase (#R010B; Takara Biomedical Technology, Beijing, China), and the target gene fragment was amplified by PCR. cDNAs encoding NLRP3 were cloned into the vector GV146 between the XhoI and EcoRI sites. The following primers were used: NLRP3 forward primer, (5'-TACCGGACTCAGATCTCGAGCGCCACCATGAAGATGGCAAGCACCCGCTGCAAG-3'); NLRP3 reverse primer (5'-TACCGTCGACTGCAGAATTCCTACCAAGAAGGCTCAAAGACGACG-3'). The resulting plasmid was used to transform cells and was verified by DNA sequencing. The transformants were transferred into LB liquid medium (10 ml) containing the corresponding antibiotics and cultured overnight at 37 °C. An EndoFree Midi Plasmid Kit (#DP118-2; Tiangen Biotech, Beijing, China) was used to carry out plasmid extraction according to the manufacturer's instructions, and the resulting preparations were used for cell transfection experiments. Empty plasmids were used controls. NLRP3 overexpression plasmids were prepared in a similar manner.

Podocyte cell culture and transfection

Conditionally immortalized human podocytes were purchased from Beina Bio (#BNCC340460; Beijing, China) and cultured in McCoy's 5A medium containing 10% fetal bovine serum (FBS) and 1% double antibody. Podocytes were cultured at 37 °C in a saturated humidified atmosphere of 5% CO_2, with culture medium replacement every 2 days using the transfection methods described above, the experimental groups were as follows: (1) control, (2) empty plasmid, (3) HBx, (4) HBx + miR-mimic, (5) HBx + miR-inhibitor, (6) HBx + miR-mimic + NLRP3, (7) HBx + miR-mimic + si-NLRP3, (8) HBx + miR-inhibitor + NLRP3, (9) HBx + miR-inhibitor+ si-NLRP3.

Immunofluorescence staining

Podocytes in 6-well plates were fixed with 4% paraformaldehyde (PFA) at room temperature for 30 min, and the slides were washed three times with PBS for 3 min. The cells were incubated in PBS containing 0.4% Triton X-100 for 10 min and blocked with 2% bovine serum albumin at 37 °C for 60 min. The cells were then incubated with the

primary antibodies anti-desmin (1:100; Boster Biological Technology, Wuhan, China) and anti-nephrin (1:100; Boster Biological Technology) at 4 °C overnight. Then, the cells were washed with PBS and incubated with anti-mouse IgG Alexa Fluor 488 or anti-rabbit IgG Alexa Fluor 594 (1:1000; Life Technologies, Paisley, UK) for 1 h at room temperature. Cells on glass cover slips were stained with 4′,6-diamidino-2-phenylindole dye (DAPI, Vector Labs, Peterborough, UK) and prepared for imaging using a fluorescence microscope (Olympus, Tokyo, Japan) (magnification, x200). In the microscopic images, desmin-positive samples were red and DAPI-positive samples were blue.

Terminal transferase dUTP nick end labeling (TUNEL) staining

A TUNEL assay (#G1501; Servicebio, Wuhan, China) was used to detect pyroptosis according to the manufacturer's instructions. Briefly, cells were fixed with 4% PFA for 30 min and then treated with 0.1% Triton X-100 for 10 min at room temperature. After washing with PBS, the cells were incubated with 50 μl TUNEL reaction mixture at 37 °C for 2 h. The nuclei were then stained with DAPI (0.3 mM) (#G1012; Servicebio) at room temperature for 10 min. After mounting with an anti-fluorescence quenching mounting medium (#G1401; Servicebio), images of cells were obtained using a Nikon Eclipse CI fluorescence microscope (Nikon, Tokyo, Japan) at a magnification of 100×. In the microscopic images, TUNEL-positive samples were green and DAPI-positive samples were blue. The percentage of positive cells was calculated as (number of cells positive/total number of cells) × 100.

Bioinformatics analysis

TargetScan 8.0 (http://www.targetscan.org/) was used to predict the target gene of miR-223.

Dual luciferase reporter assay

The promoter sequence of NLRP3 was cloned into the psi-CHECK2 vector (Promega, Madison, WI, USA) upstream of the luciferase sequence. Podocytes at a density of 20,000 cells per well were seeded in 96-well plates. The podocytes were cotransfected with miR-223 mimic or miR-NC along with luciferase reporters containing the wild-type (WT) or mutant (MUT) 3'-untranslated region (3'-UTR) sequence of NLRP3. Lipofectamine 2000 was used as the transfection reagent. After 48 h of incubation, the podocytes were harvested. Luciferase activity was analyzed using the Dual-Luciferase Reporter Assay System (Promega, Madison, WI, USA) according to the manufacturer's instructions.

Hoechst 33342 staining

The numerical and morphological changes of nuclei were observed by staining the nucleus with Hoechst 33342 (#C0030; Solarbio, Beijing, China). The podocytes transfected with different vectors were stained with Hoechst 33342 and cultured in an incubator for 20-30 min, after which the medium was discarded and the cells were washed 2-3 times with medium. The cells were then imaged under a fluorescence microscope (Olympus, Tokyo, Japan), using five random fields (magnification, 400×), and immediately processed in Adobe Photoshop CS5 (Adobe Systems, USA).

qRT-PCR analysis

Total RNA was extracted from cells using TRIzol Reagent (Tiangen Biotech, Beijing, China) and was reverse transcribed into cDNA using a SuperScript Reverse Transcription Kit (Tiangen Biotech). Subsequently, PCR was performed using the resulting cDNAs and SYBR Green Master Mix (Tiangen Biotech) according to the manufacturer's instructions. Glyceraldehyde 3-phosphate dehydrogenase (GAPDH) and β-actin served as internal controls. The qRT-PCR was repeated three times. The relative mRNA expression levels were determined using the $2^{-\Delta\Delta Ct}$ method. The primers used are shown in Table 1.

Western blot (WB) analysis

Proteins were extracted from podocytes using radioimmunoprecipitation assay (RIPA) lysis buffer (Boster Biological Technology, Wuhan, China), and their concentration was determined using a BCA assay (Boster Biological Technology). After denaturation, the proteins were separated by sodium dodecyl sulfate-polyacrylamide gel electrophoresis (SDS-PAGE; Servicebio) and transferred to a polyvinylidene difluoride (PVDF) membrane (Millipore, Billerica, MA, USA). The membranes were blocked in 5% skimmed milk at room temperature for 1 h and then incubated overnight at 4 °C with the primary antibodies specific for NLRP3 (1:1000; Proteintech, Chicago, USA), caspase-1, ASC, IL-1β, IL-18 (1:1000; ABclonal Biotechnology, Wuhan, China), and GAPDH (1:5000; Proteintech, Chicago, USA). The membranes were washed three times with TBST and incubated with HRP-labelled goat anti-rabbit or anti-mouse IgG (1:5000; ZSGB Biotech, Beijing, China) for 1 h. After incubation at room temperature for 1 h, the membranes were washed three times with TBST. Finally, the resulting bands were detected using enhanced chemiluminescence (ECL) reagents (Servicebio, Wuhan, China), and signal intensity was quantified using greyscale analysis software (ImageJ 3.00).

Table 1 Primers used in qRT-PCR

Gene	Forward primer	Reverse primer
HBx	GAAAACACACTCACTGTTCAGAG	GTAAGCCGCTTTCTCTTATGCAG
miR-223	GCTTGTACATGGTAGGCTT	CAGTGCGTGTCGTGGAGT
NLRP3	GCGCCTCAGTTAGAGGATGT	ACCAGCTACAAAAAGCATGGA
ASC	GATCCAGGCCCCTCCTCA	AAGAGCTTCCGCATCTTGCT
Caspase-1	GCCTGTTCCTGTGATGTGGA	CTTCACTTCCTGCCCACAGA
IL-1β	AGCTCGCCAGTGAAATGATGG	TAGTGGTGGTCGGAGATTCG
IL-18	CGCTTCCTCTCGCAACAAAC	ATTCCAGGTTTTCATCATCTTCAGC
β-actin	ACAACCTTCTTGCAGCTCCTC	AATGCCGTGTTCAATGGGGT
GAPDH	AGAAGGCTGGGGCTCATTTG	AGGGGCCATCCACAGTCTTC

Flow cytometry assay

Cell pyroptosis was further analyzed by flow cytometry using an *In Situ* Cell Death Detection Kit (Immunochemistry, Bloomington, USA) according to the manufacturer's instructions. Podocytes were cultured in 6-well plates and divided into nine groups as described above. After transfection, the podocytes were digested and collected in tubes. The supernatant was discarded after centrifugation, and the cells were washed three times and then double-stained with annexin V-fluorescein isothiocyanate and propidium iodide at room temperature for 15 min in the dark. The results were analyzed using flow cytometry, and the pyroptosis rate was calculated as the percentage of early and late pyroptosis cells.

Measurement of caspase-1 activity

To determine the activity of caspase-1 in different groups, the cells were analyzed using a Caspase-1 Activity Assay Kit (#MA0327; Meilun Biotechnology Co., Ltd., Dalian, China) according to the manufacturer's instructions. This kit is based on the fact that caspase-1 can catalyze the production of yellow *p*-nitroaniline (pNA) from the substrate acetyl-pyrVal-Ala-Asp *p*-nitroanilide (Ac-YVAD-pNA). Therefore, the activity of caspase-1 can be detected by measuring the absorbance of pNA using a standard pNA curve. Podocytes were collected, and the Bradford method was used to determine the protein concentration. Fifty μL of each sample was incubated overnight at 37 °C in a 96-well microtiter plate with 10 μL of Ac-YVAD-pNA (2 mM). The absorbance of pNA was measured at 405 nm using a microplate reader. Finally, the detection of pNA production in the samples indicated the level of caspase-1 activation.

Statistical analysis

Measurement data are expressed as the mean ± standard deviation and were further analyzed using GraphPad Prism 8.0. For normally distributed data, an unpaired *t*-test was used to compare two groups. All experiments were performed at least three times. Statistical significance was set at a p-value < 0.05.

Results

miR-223 is downregulated in podocytes exposed to HBx

As a first step, HBx-overexpressing lentiviruses were introduced into podocytes by transfection (Fig. 1A). Previous studies have shown that miR-223 is downregulated in cases of hepatitis B [16]. To evaluate its role in HBx-transfected podocytes, qRT-PCR was performed to measure the expression of miR-223. As shown in Figure 1B, miR-223 was downregulated in HBx-transfected podocytes, indicating that it may play a role in HBx-induced podocyte injury ($p < 0.05$).

HBx induces podocyte pyroptosis through the NLRP3 inflammasome

In our previous study, we demonstrated that NLRP3 plays a crucial role in the process of HBx-induced pyroptosis [17]. To further investigate the mechanism of HBx-induced podocyte injury, TUNEL and immunofluorescence staining were used to observe pyroptosis-related cell death. In the TUNEL assay, we observed elevated TUNEL-positive podocytes (green) in the HBx group compared to the control group, which was successfully suppressed by the introduction of si-NLRP3 ($p < 0.05$; Fig. 2A-B). Immunofluorescence staining revealed that HBx increased the expression of desmin, a marker of cell necrosis, and this was notably alleviated by introduction of

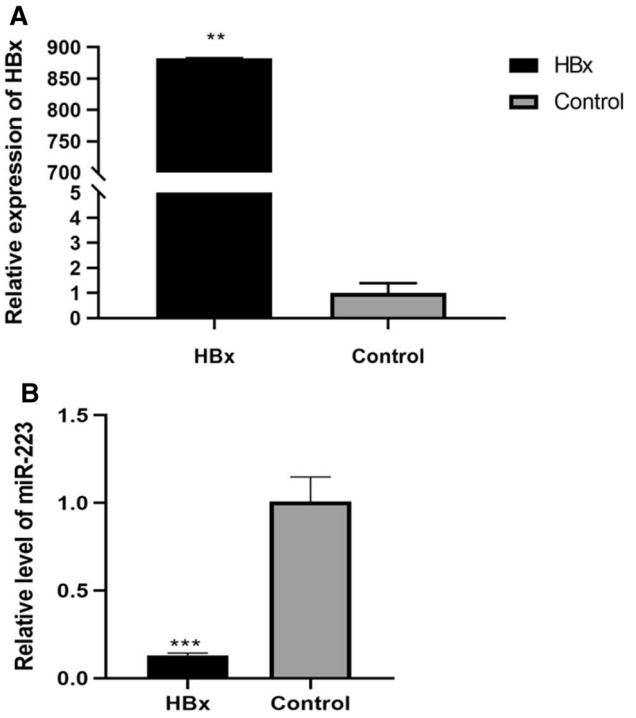

Fig. 1 miR-223 is downregulated in podocytes exposed to HBx (n = 3). (A) HBx and (B) miR-223 expression were measured by RT-PCR. The data are presented as the mean ± SD. **, $p < 0.01$; ***, $p < 0.001$ versus the control

si-NLRP3 (Fig. 2C). As expected, the opposite effect was observed with nephrin (Fig. 2D). Taken together, these findings indicate the involvement of the NLRP3 inflammasome in the pathogenesis of HBx-induced pyroptosis.

NLRP3 is a direct target of miR-223

It has been reported that NLRP3 inflammasomes in kidney diseases are mainly activated through the canonical pathway involving caspase-1, which results in podocyte pyroptosis [18]. To better elucidate the effect of miR-223 downregulation on podocyte pyroptosis, target prediction programs were used to predict targets of miR-223, and NLRP3 was found to be a potential target (Fig. 3A). We then tested whether NLRP3 was a direct target of miR-223 in HBV-GN using a dual-luciferase assay. The results showed that the miR-223 agomir significantly inhibited the luciferase activity of NLPR3 (wild-type [WT]) reporters, whereas miR-223 overexpression had little effect on luciferase activity when the binding sites of miR-223 and NLRP3 were mutated (Fig. 3B). These data demonstrated that miR-223 binds directly to the NLRP3 3'-UTR to inhibit its expression.

NLPR3 overexpression impairs the protective activity of miR-223 in podocyte injury

To examine the effect of miR-223 on the NLRP3 inflammasome (NLRP3, caspase-1, and ASC) and its released inflammatory factors (IL-1β and IL-18) in podocyte pyroptosis, we performed rescue experiments with miR-223 and NLRP3 inflammasomes. WB was performed to analyze the expression of NLRP3, caspase-1, ASC, IL-1β, and IL-18 in each group (Fig. 4A). As shown in Figure 4B, compared with the control group, the level of NLRP3 decreased significantly after treatment with an miR-223 mimic ($p < 0.05$), whereas the effect was aggravated when NLRP3 was overexpressed ($p < 0.05$). Similar results were obtained for caspase-1, ASC, and IL-1β ($p < 0.05$; Fig. 4C, D, and E). There was no significant change In IL-18 protein expression after overexpression of NLRP3 ($p > 0.05$; Fig. 4F). Therefore, increasing the level of NLRP3 inflammasomes limited the decrease in pyroptosis-related proteins by miR-223. Taken together, our data suggest that NLPR3 overexpression lessens the effect of miR-223 on podocyte pyroptosis.

HBx mediates podocyte pyroptosis through miR-223 and the NLRP3 inflammasome

We have already demonstrated decreased expression of miR-223 in HBx-transfected podocytes and the negative regulatory relationship between miR-223 and NLRP3 inflammasomes, but it remains unclear whether HBx mediates podocyte pyroptosis through the miR-223/NLRP3 axis. To better understand the molecular mechanism involved, miR-223 mimics and inhibitors were used to interfere with miR-223 expression. In addition, the effect of NLRP3 plasmids or si-NLRP3 on the level of NLRP3 was analyzed using qRT-PCR and WB (Fig. 5). The qRT-PCR results showed that the level of NLRP3 mRNA was higher in the HBx group than in the control and empty plasmid groups. However, the expression of NLRP3 decreased in the HBx + miR-mimic and HBx + miR-mimic + si-NLRP3 groups. In addition, miR-223 inhibitors upregulated NLRP3 significantly in HBx-induced podocytes compared with the HBx group ($p < 0.05$; Fig. 5A). Similar results were observed for caspase-1, ASC, IL-1β, and IL-18 (Fig. 5B-E). These results were confirmed by WB experiments (Fig. 5F), which showed that the expression of the NLRP3 inflammasome and its inflammatory cytokines were increased in the HBx group, while treatment with the miR-223 mimic and si-NLRP3 reduced the level of inflammatory cytokines significantly. In addition, the level of IL-18 was higher in the HBx + miRNA inhibitor + NLRP3 group than in the HBx group ($p < 0.05$; Fig. 5J-K). However, there was no statistical difference in the quantitative analysis results for ASC

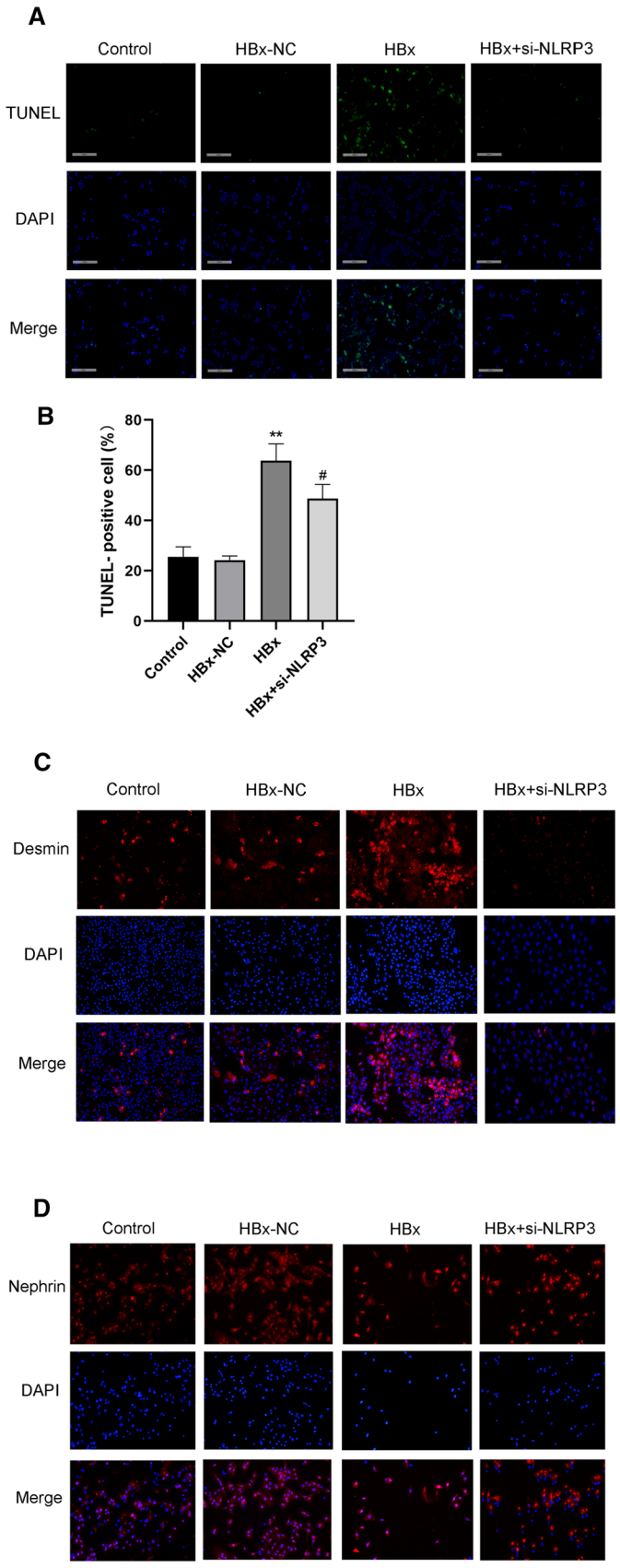

Fig. 2 HBx induces podocyte pyroptosis through NLRP3 inflammasomes (n = 3). (A) Representative photomicrographs of TUNEL staining (scale bar, 100 μm) (×100). (B) Quantitative analysis of TUNEL-positive cells in each group. Desmin (C) and nephrin (D) expression were detected by immunofluorescence (×200). NC, negative control; si, small interfering RNA. The data are presented as the mean ± SD. **, $p < 0.01$ versus control, #, $p < 0.05$ versus the HBx group

A

	Predicted consequential pairing of target region (top) and miRNA (bottom)	Site type	Context++ score	Context++ score percentile	Weighted context++ score	Conserved branch length	P_{CT}
Position 406-412 of NLRP3 3' UTR	5' ...CGCUAUCUUUCUAUUAACUGACC...	7mer-m8	-0.30	94	-0.30	3.188	0.33
hsa-miR-223-3p	3' ACCCCAUAAACUGU-UUGACUGU						

B

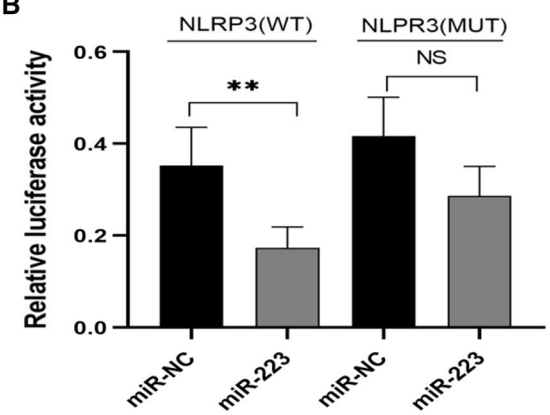

Fig. 3 NLRP3 is a direct target of miR-223. (A) Binding sites between miR-223 and the 3′-untranslated region of NLRP3 were analyzed using bioinformatics methods. (B) Effect of miR-223 upregulation on luciferase activity of NLRP3 (WT) or NLRP3 (MUT) reporter, measured using the luciferase reporter assay system (n = 3). WT, wild-type; MUT, mutant; NC, negative control. The data are presented as the mean ± SD. **, $p < 0.01$ versus miR-NC

($p > 0.05$; Fig. 5I). The gene expression of ASC in some diseases has been reported to be slightly different from that of caspase-1, indicating that it may be independent of the expression of the NLRP3 inflammasome [19], which may be one of the factors that affected our experimental results. Subsequently, we assessed the enzyme activity of caspase-1 and found that it was significantly higher in the HBx + miRNA inhibitor + NLRP3 transfection group than in the HBx group ($p < 0.05$; Fig. 5L).

In order to further explore the relationship between the miR-223/NLRP3 axis and podocyte pyroptosis, flow-cytometry-based pyroptosis detection and Hoechst 33342 staining were performed. Compared with the control group and the empty plasmid group, the level of cell pyroptosis was significantly higher in the HBx groups. However, cell pyroptosis significantly decreased in the HBx + miR-mimic + si-NLRP3 group, indicating that the miR-223/NLRP3 axis plays a critical role in HBx-induced pyroptosis ($p < 0.05$; Fig. 5M). Hoechst 33342 staining showed that the nuclei of podocytes were densely stained and that the chromatin was more condensed in the HBx group than in the control group and the empty plasmid group, and this was reversed by treatment with miR-223 and si-NLRP3 (Fig. 5N). These results suggest that HBx-induced pyroptosis is associated with downregulation of miR-223 via the NLRP3 pathway.

Discussion

In the present study, we found that the expression of miR-223 was downregulated in podocytes exposed to HBx. Moreover, our results confirmed that expression of the HBx protein in podocytes induced pyroptosis. HBx-induced podocyte models were established in order to investigate the role of miR-223 in HBx-induced pyroptosis and to test whether activation of the NLRP3 inflammasome is involved in the underlying mechanism.

HBV-GN is one of the most common extrahepatic manifestations in patients with chronic HBV infection [20]. A large number of studies on the HBx gene, one of the four genes of HBV, have been performed since the establishment of HBx transgenic mice [21]. However, there are various mechanisms of HBx-induced podocyte injury in human kidney diseases, such as inflammatory response and oxidative stress, and the former may be of great importance. The NLRP3 inflammasome, composed of NLRP3, ASC, and pro-caspase-1, is closely associated with the innate immune system. Activated caspase-1 cleaves full-length gasdermin D (GSDMD) to form a gasdermin pore, which allows the release of proinflammatory cytokines pro-IL-1β and pro-IL-18, leading to cell swelling and dissolution [22]. It is the characteristic cascade inflammatory response of pyroptosis that sets it apart from apoptosis and necrosis. Stimuli

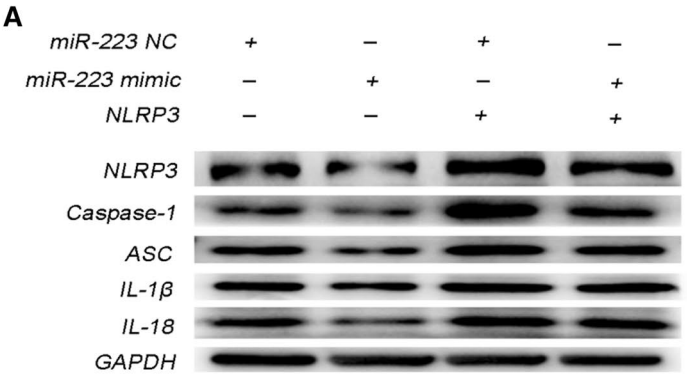
A
miR-223 NC + − + −
miR-223 mimic − + − +
NLRP3 − − + +
NLRP3
Caspase-1
ASC
IL-1β
IL-18
GAPDH

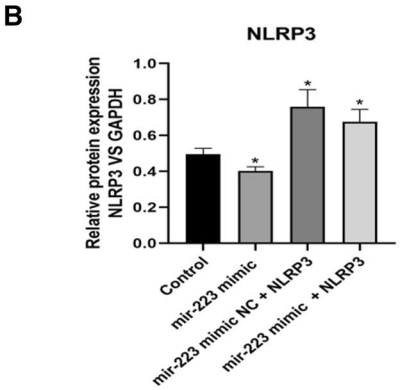
B
NLRP3
Relative protein expression NLRP3 VS GAPDH
1.0
0.8
0.6
0.4
0.2
0.0
Control
mir-223 mimic
mir-223 mimic NC + NLRP3
mir-223 mimic + NLRP3

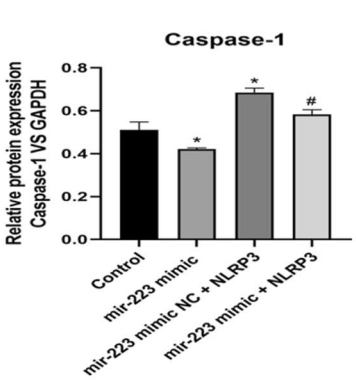
C
Caspase-1
Relative protein expression Caspase-1 VS GAPDH
0.8
0.6
0.4
0.2
0.0
Control
mir-223 mimic
mir-223 mimic NC + NLRP3
mir-223 mimic + NLRP3

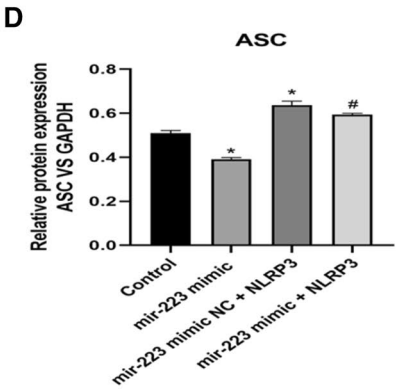
D
ASC
Relative protein expression ASC VS GAPDH
0.8
0.6
0.4
0.2
0.0
Control
mir-223 mimic
mir-223 mimic NC + NLRP3
mir-223 mimic + NLRP3

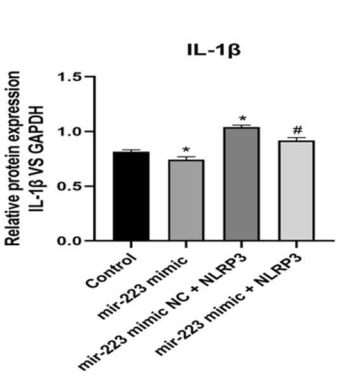
E
IL-1β
Relative protein expression IL-1β VS GAPDH
1.5
1.0
0.5
0.0
Control
mir-223 mimic
mir-223 mimic NC + NLRP3
mir-223 mimic + NLRP3

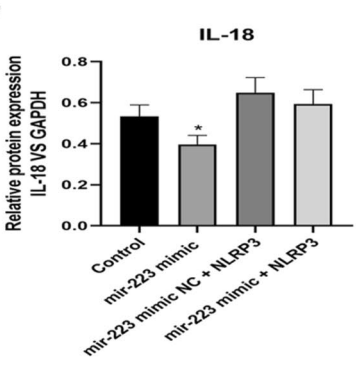
F
IL-18
Relative protein expression IL-18 VS GAPDH
0.8
0.6
0.4
0.2
0.0
Control
mir-223 mimic
mir-223 mimic NC + NLRP3
mir-223 mimic + NLRP3

◂**Fig. 4** NLPR3 overexpression decreases the protective effect of miR-223 in podocyte injury (n = 3). (A) Western blot analysis showing the protein levels of the pyroptosis-associated markers NLRP3, ASC, caspase-1, IL-1β, and IL-18. (B-F) Western blot showing the relative expression of NLRP3, caspase-1, ASC, IL-1β, and IL-18. NC, negative control; miR-mimic, miR-223 mimic; miR-inhibitor, miR-223 inhibitor. The data are presented as the mean ± SD. *, $p < 0.05$ versus control; #, $p < 0.05$ versus the miR-223 mimic NC+NLRP3 group

such as CD36 and nicotine induce reactive oxygen species production and then activate the NLRP3 inflammasome to induce the inflammatory response and cell damage [23, 24]. Mutations in NLRP3-inflammasome receptors trigger autoimmune diseases, and imbalanced activity is associated with the pathological process of many diseases [25]. NLRP3 inflammasome-mediated pyroptosis induced by a variety of stimulus occurs in Alzheimer's disease, atherosclerosis, diabetes mellitus, glomerular inflammatory diseases, renal ischemia reperfusion injury, and podocyte injury [26–31]. A study has shown that pyroptosis can be used against cancer by induction in tumor cells [32]. Therefore, we speculate that pyroptosis may play a pivotal role in HBx-induced podocyte injury and that the NLRP3 inflammasome may be a new therapeutic target for HBV-GN.

miRNAs are normally extended by adding stem-loop primers or 3′ adenylation for traditional PCR detection [33]. Although the detection of miRNAs is very challenging, it has become an important focus of our research on disease mechanisms. For example, miRNAs participate in cancer initiation and metastasis [34], and upregulation of miR-125b is associated with severe liver fibrosis of patients with chronic hepatitis C [35]. miRNAs also play an important role in kidney disease. In acute kidney injury, some miRNAs influence renal function through cell apoptosis [36]. miR-155 influences the release of proinflammatory factors in early renal disease [37]. Previous studies confirmed that miR-223 may act as a negative regulator in the inflammatory process of viral hepatitis [38]. Therefore, we hypothesized that miR-223 has a similar regulatory effect on podocyte damage in HBV-GN. miR-223 was first discovered in the hematopoietic system [39] and has also been shown to limit liver fibrosis and reduce urate-induced gouty inflammation and cardiovascular damage [8, 40, 41]. Interestingly, the inflammatory response in diseases caused by miR-223 downregulation always seems to be accomplished by targeting the NLRP3 inflammasome [8, 40]. In this study, we found that miR-223 downregulation in HBx-induced podocytes is associated with pyroptosis. Therefore, we tested HBx-induced pyroptosis after transfection with miR-223 mimics and found that miR-223 upregulation decreased the expression of NLRP3. Moreover, transfection with miR-223 mimics downregulated the expression of ASC, caspase-1, IL-1β, and IL-18. These results indicate that downregulation of miR-223 increases the expression of the NLRP3 inflammasome, which is consistent with the results of Bauernfeind et al. [42].

Studies on the mechanisms of miRNAs provide new insights for the diagnosis and treatment of many clinical diseases. To better understand the mechanism of HBV-GN, we examined the expression of pyroptosis-related proteins exposed to HBx and NLRP3 or si-NLRP3 in the presence of miR-223 mimics or inhibitors. Compared with the HBx group, the HBx + miRNA inhibitor + NLRP3 transfection group exhibited more-severe features of pyroptosis. It has been suggested that the detection of characteristic miRNAs in serum could be used to predict tumor recurrence and survival rates of patients with triple-negative breast cancer [43]. In treatment, miRNAs are chemically modified or delivered as vectors to reduce RNase interference [44]. miRNAs are also packaged into multivesicular bodies with hormone-like effects and function as anticancer drug targets [45]. Based on these studies, miR-223 may be a novel diagnosis and treatment target for HBV-GN.

Our research first demonstrated that miR-223 plays a role in HBx-protein-mediated podocyte pyroptosis by targeting the NLRP3 inflammasome. However, the present study has limitations. First, we only performed relevant cellular experiments without validation in mouse models and clinical cases. Second, the regulation of HBx, miR-223, and NLRP3 inflammasome is particularly complex, and we did not analyze whether other genes are involved. Further studies on the mechanism of HBV-GN should therefore be performed.

In conclusion, we report that the HBx protein can induce pyroptosis of human kidney podocytes in HBV-GN and that miR-223 plays a protective role in the pathogenesis of the disease. miR-223 negatively regulates the expression of the NLRP3 inflammasome, which is involved in the pathogenesis of HBV-GN. More importantly, the findings of this study may provide novel insights into the potential use of miRNAs in the diagnosis and treatment of kidney disease.

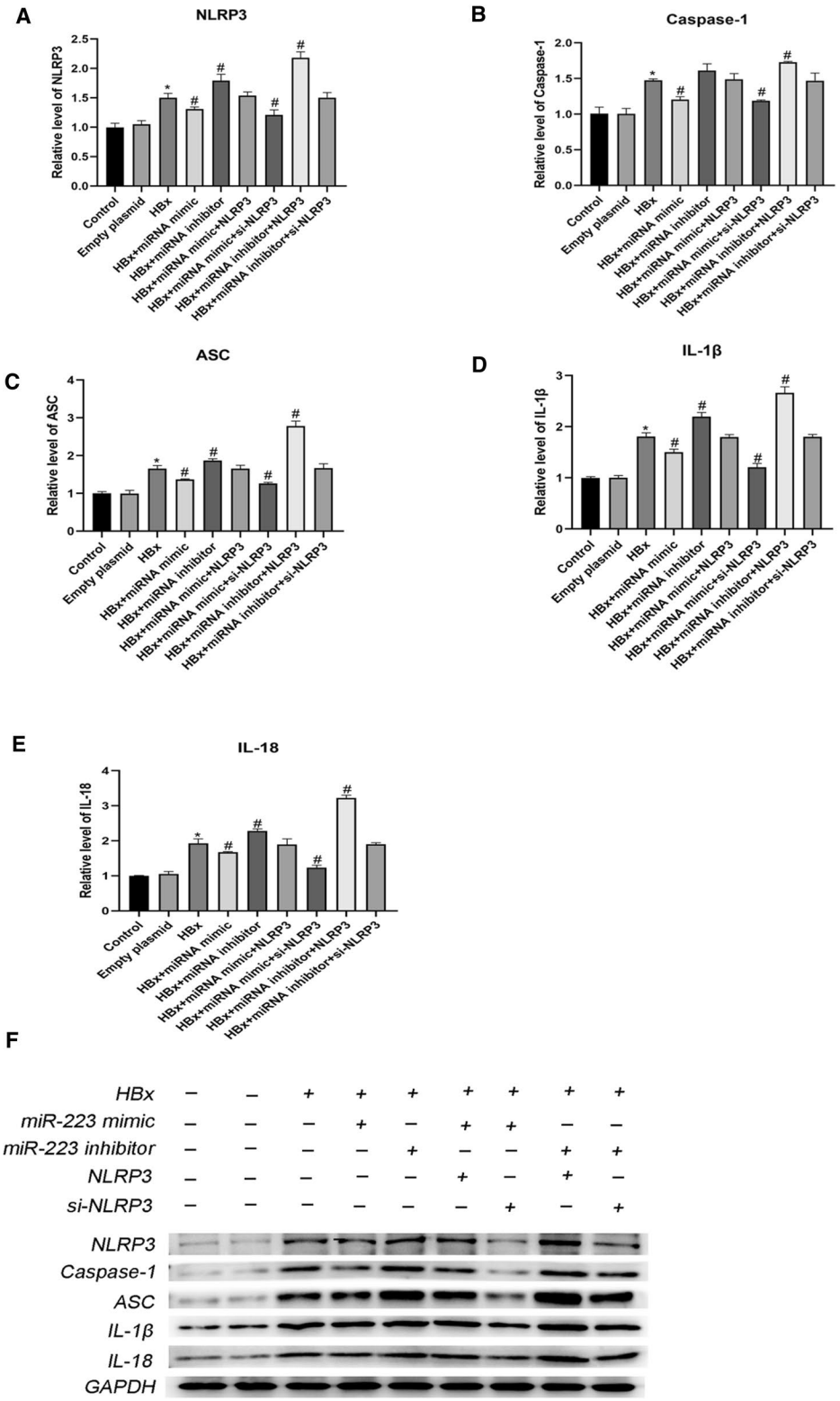

Fig. 5 HBx mediates podocyte pyroptosis through miR-223 and the NLRP3 inflammasome (n = 3). (A-E) RT-PCR assay showing the relative levels of NLRP3, caspase-1, ASC, IL-1β, and IL-18. (F-K) Western blot analysis showing the protein levels of NLRP3, caspase-1, ASC, IL-1β, and IL-18. (L) Caspase-1 enzyme activity measured by ELISA. (M) Flow cytometry analysis of pyroptosis in each group. (N) Fluorescence microscopy (×400) results of each group. miR-mimic, miR-223 mimic; miR-inhibitor, miR-223 inhibitor; si, small interfering RNA. The data are presented as the mean ± SD. *, $p < 0.05$ versus the control and empty plasmid groups; #, $p < 0.05$ versus the HBx group

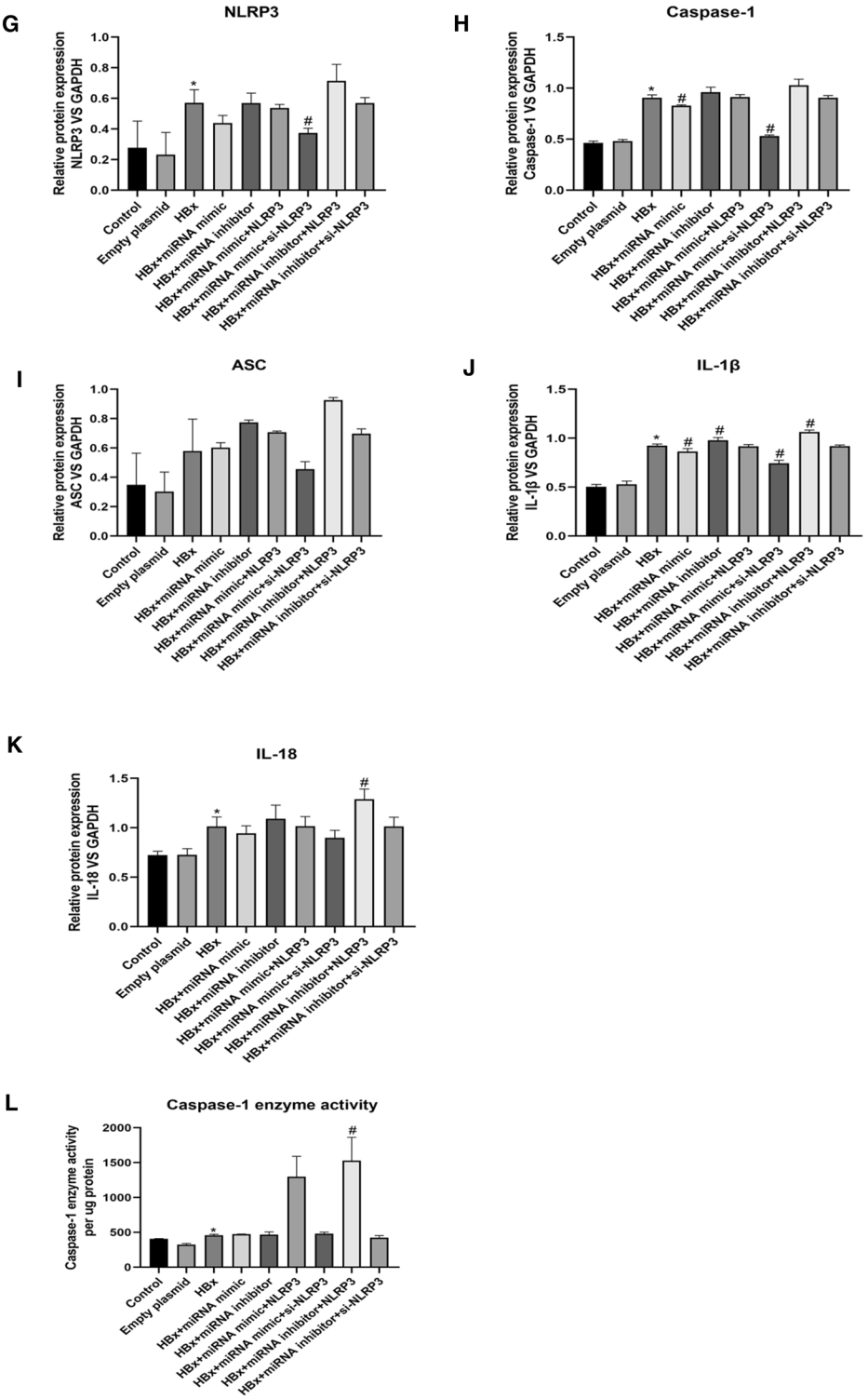

Fig. 5 (continued)

Fig. 5 (continued)

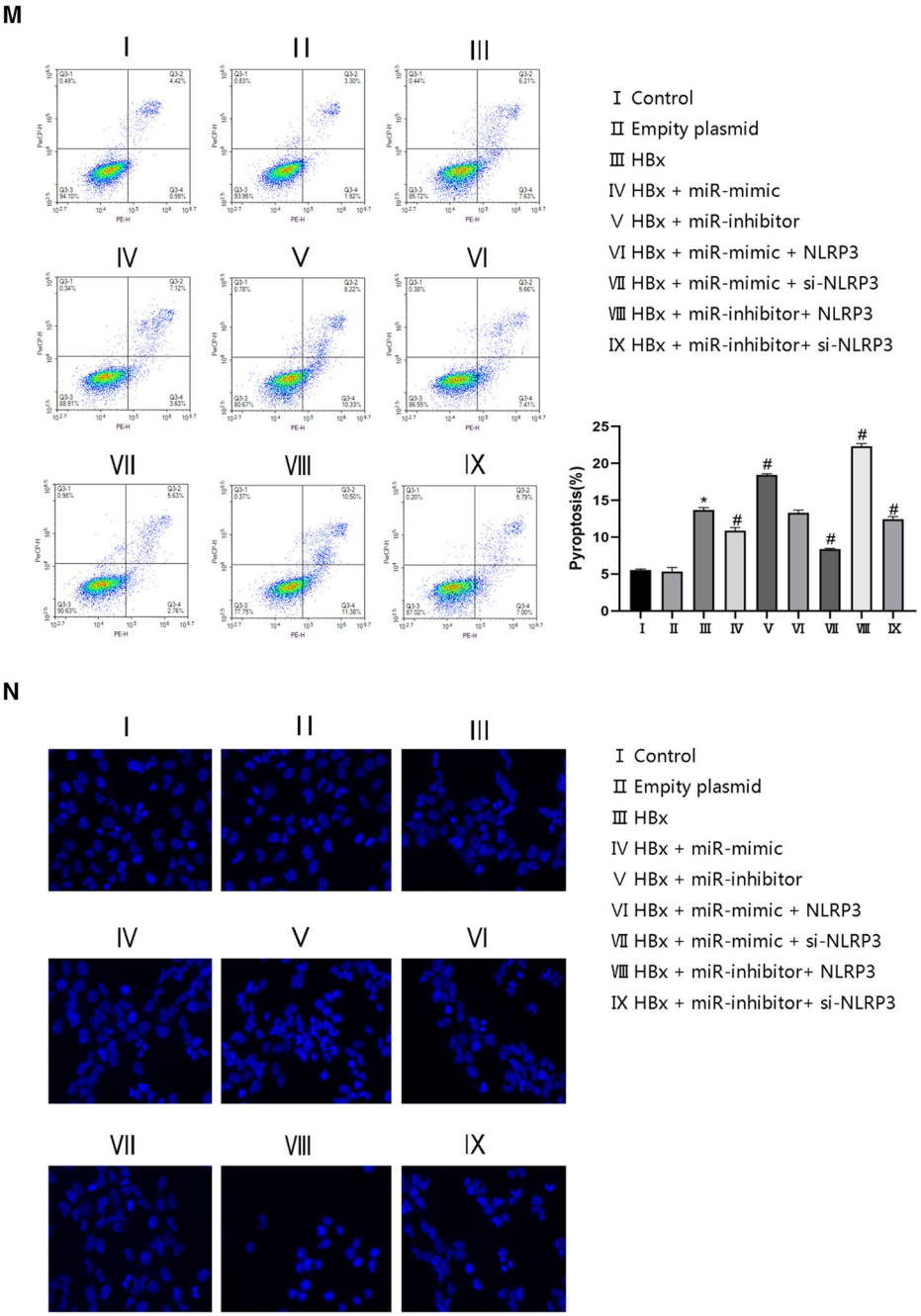

Author contributions Yani YU, Hui DONG, and Wei JIANG designed the experimental idea and wrote the main manuscript text. Yue ZHANG, Jingyi SUN, and Baoshuang LI performed the experiments and collected the relevant data. Yueqi CHEN, Moxuan FENG, and Xiaoqian YANG finished the formal analysis and investigation. Shengbo GAO prepared Figures 1-5. All authors reviewed the manuscript.

Funding This work was supported by the National Natural Science Foundation of China (grant number NSFC 81870494), the Chinese Society of Nephrology (grant number 20010080800), and the Qingdao Outstanding Health Professional Development Fund (grant number 2020-2022).

Declarations

Conflict of interest None.

Ethical approval Approval was granted by the Affiliated Hospital of Qingdao University. All methods were performed in accordance with the relevant guidelines and regulations.

References

1. Jiang W, Liu T, Dong H et al (2015) Relationship between serum DNA replication, clinicopathological characteristics and prognosis of hepatitis B virus-associated glomerulonephritis with severe proteinuria by lamivudine plus adefovir dipivoxil combination therapy. Biomed Environ Sci 28:206–213
2. Diao Z, Ding J, Yin C et al (2013) Purified hepatitis B virus induces human mesangial cell proliferation and extracellular matrix expression in vitro. Virol J 10:300
3. Dong H, Xu Y, Jiang W et al (2014) Significance of mutations in hepatitis B virus X gene for the pathogenesis of HB-associated glomerulonephritis. Acta Virol 58:278–281
4. Latz E, Xiao TS, Stutz A (2013) Activation and regulation of the inflammasomes. Nat Rev Immunol 13:397–411
5. Zhang X, Dong P, Xu L et al (2019) The different expression of caspase-1 in HBV-related liver disease and acts as a biomarker for acute-on-chronic liver failure. BMC Gastroenterol 19:148
6. Zuo W, Tian R, Chen Q et al (2021) miR-330-5p inhibits NLRP3 inflammasome-mediated myocardial ischaemia–reperfusion injury by targeting TIM3. Cardiovasc Drugs Ther 35:691–705
7. Zhang H, Du Y, Guo Y et al (2021) TLR4-NLRP3-GSDMD-mediated pyroptosis plays an important role in aggravated liver injury of CD38 sepsis mice. J Immunol Res 2021:6687555
8. Zhang Q, Zhu D, Dai F et al (2021) MicroRNA-223 suppresses IL-1β and TNF-α production in gouty inflammation by targeting the NLRP3 inflammasome. Front Pharmacol 12:637415
9. Vilaysane A, Chun J, Seamone ME et al (2010) The NLRP3 inflammasome promotes renal inflammation and contributes to CKD. J Am Soc Nephrol 21:1732–1744
10. Si J, Yu C, Guo Y et al (2018) Chronic hepatitis B virus infection and risk of chronic kidney disease: a population-based prospective cohort study of 0.5 million Chinese adults. BMC Med 16:93
11. Ameres SL, Zamore PD (2013) Diversifying microRNA sequence and function. Nat Rev Mol Cell Biol 14:475–488
12. Lui JC (2017) Regulation of body growth by microRNAs. Mol Cell Endocrinol 456:2–8
13. Ojha CR, Rodriguez M, Dever SM et al (2016) Mammalian microRNA: an important modulator of host-pathogen interactions in human viral infections. J Biomed Sci 23:74
14. Cortez MA, Bueso-Ramos C, Ferdin J et al (2011) MicroRNAs in body fluids—the mix of hormones and biomarkers. Nat Rev Clin Oncol 8:467–477
15. Ishii H, Kaneko S, Yanai K et al (2020) MicroRNAs in podocyte injury in diabetic nephropathy. Front Genet 11:993
16. Haneklaus M, Gerlic M, O'Neill LA et al (2013) miR-223: infection, inflammation and cancer. J Intern Med 274:215–226
17. Yu Y, Dong H, Sun J et al (2022) Hepatitis B virus X mediates podocyte pyroptosis by regulating the ROS/NLRP3 signaling pathway in hepatitis B virus-associated glomerulonephritis. Iran J Basic Med Sci 25:103–109
18. Xiang H, Zhu F, Xu Z et al (2020) Role of inflammasomes in kidney diseases via both canonical and non-canonical pathways. Front Cell Dev Biol 8:106
19. Stienstra R, van Diepen JA, Tack CJ et al (2011) Inflammasome is a central player in the induction of obesity and insulin resistance. Proc Natl Acad Sci USA 108:15324–15329
20. Liao MT, Chang MH, Lin FG et al (2011) Universal hepatitis B vaccination reduces childhood hepatitis B virus-associated membranous nephropathy. Pediatrics 128:e600–e604
21. Yu DY, Moon HB, Son JK et al (1999) Incidence of hepatocellular carcinoma in transgenic mice expressing the hepatitis B virus X-protein. J Hepatol 31:123–132
22. Fischer FA, Chen KW, Bezbradica JS (2021) Posttranslational and therapeutic control of gasdermin-mediated pyroptosis and inflammation. Front Immunol 12:661162
23. Hou Y, Wang Q, Han B et al (2021) CD36 promotes NLRP3 inflammasome activation via the mtROS pathway in renal tubular epithelial cells of diabetic kidneys. Cell Death Dis 12:523
24. Singh GB, Kshirasagar N, Patibandla S et al (2019) Nicotine instigates podocyte injury via NLRP3 inflammasomes activation. Aging (Albany NY) 11:12810–12821
25. Awad F, Assrawi E, Louvrier C et al (2018) Inflammasome biology, molecular pathology and therapeutic implications. Pharmacol Ther 187:133–149
26. Lei B, Liu J, Yao Z et al (2021) viaNF-κB-induced upregulation of miR-146a-5p promoted hippocampal neuronal oxidative stress and pyroptosis TIGAR in a model of Alzheimer's disease. Front Cell Neurosci 15:653881
27. Yin R, Zhu X, Wang J et al (2019) MicroRNA-155 promotes the ox-LDL-induced activation of NLRP3 inflammasomes via the ERK1/2 pathway in THP-1 macrophages and aggravates atherosclerosis in $ApoE^{-/-}$ mice. Ann Palliat Med 8:676–689
28. Xu D, Zhang X, Chen X et al (2020) Inhibition of miR-223 attenuates the NLRP3 inflammasome activation, fibrosis, and apoptosis in diabetic cardiomyopathy. Life Sci 256:117980
29. Hong J, Bhat OM, Li G et al (2019) Lysosomal regulation of extracellular vesicle excretion during d-ribose-induced NLRP3 inflammasome activation in podocytes. Biochim Biophys Acta Mol Cell Res 1866:849–860
30. Wu H, Huang T, Ying L et al (2016) MiR-155 is involved in renal ischemia-reperfusion injury via direct targeting of FoxO3a and regulating renal tubular cell pyroptosis. Cell Physiol Biochem 40:1692–1705
31. Zhang Q, Conley SM, Li G et al (2019) Rac1 GTPase inhibition blocked podocyte injury and glomerular sclerosis during hyperhomocysteinemia via suppression of nucleotide-binding oligomerization domain-like receptor containing pyrin domain 3 inflammasome activation. Kidney Blood Press Res 44:513–532
32. Tan Y, Chen Q, Li X et al (2021) Pyroptosis: a new paradigm of cell death for fighting against cancer. J Exp Clin Cancer Res 40:153
33. Lu TX, Rothenberg ME (2018) MicroRNA. J Allergy Clin Immunol 141:1202–1207
34. Kim J, Yao F, Xiao Z et al (2018) MicroRNAs and metastasis: small RNAs play big roles. Cancer Metastasis Rev 37:5–15
35. Sultana C, Rosca A, Ruta S (2019) Correlation between miR-125b expression and liver fibrosis in patients with chronic hepatitis C. Hepat Mon 19:e84615
36. Zankar S, Trentin-Sonoda M, Viñas JL et al (2021) Therapeutic effects of micro-RNAs in preclinical studies of acute kidney injury: a systematic review and meta-analysis. Sci Rep 11:9100
37. Zheng X, Zhong Q, Lin X et al (2021) Transforming growth factor-β1-induced podocyte injury is associated with increased microRNA-155 expression, enhanced inflammatory responses and MAPK pathway activation. Exp Ther Med 21:620
38. Ye D, Zhang T, Lou G et al (2018) Role of miR-223 in the pathophysiology of liver diseases. Exp Mol Med 50:1–12
39. Johnnidis JB, Harris MH, Wheeler RT et al (2008) Regulation of progenitor cell proliferation and granulocyte function by microRNA-223. Nature 451:1125–1129
40. Wang X, Seo W, Park SH et al (2021) MicroRNA-223 restricts liver fibrosis by inhibiting the TAZ-IHH-GLI2 and PDGF signaling pathways via the crosstalk of multiple liver cell types. Int J Biol Sci 17:1153–1167
41. Maruyama D, Kocatürk B, Lee Y et al (2021) MicroRNA-223 Regulates the development of cardiovascular lesions in LCWE-induced murine Kawasaki disease vasculitis by repressing the NLRP3 inflammasome. Front Pediatr 9:662953

42. Bauernfeind F, Rieger A, Schildberg FA et al (2012) NLRP3 inflammasome activity is negatively controlled by miR-223. J Immunol 189:4175–4181
43. Kleivi SK, Bottai G, Naume B et al (2015) A serum microRNA signature predicts tumor relapse and survival in triple-negative breast cancer patients. Clin Cancer Res 21:1207–1214
44. Lai X, Eberhardt M, Schmitz U et al (2019) Systems biology-based investigation of cooperating microRNAs as monotherapy or adjuvant therapy in cancer. Nucleic Acids Res 47:7753–7766
45. Ling H, Fabbri M, Calin GA (2013) MicroRNAs and other non-coding RNAs as targets for anticancer drug development. Nat Rev Drug Discov 12:847–865